Publications

Department of Physics

6-2007

Large Magnetic Entropy Change in Ni50Mn50–xInx Heusler Alloys

Arjun Kumar Pathak
Southern Illinois University Carbondale

Mahmud Khan
Southern Illinois University Carbondale

Igor Dubenko
Southern Illinois University Carbondale

Shane Stadler
Southern Illinois University Carbondale

Naushad Ali
Southern Illinois University Carbondale

Recommended Citation

Large magnetic entropy change in Ni$_{50}$Mn$_{50-x}$In$_x$ Heusler alloys

Arjun Kumar Pathak,[a)] Mahmud Khan, Igor Dubenko, Shane Stadler, and Naushad Ali

Department of Physics, Southern Illinois University, Carbondale, Illinois 62901

The magnetocaloric properties of polycrystalline Ni$_{50}$Mn$_{50-x}$In$_x$ ($15 \leqslant x \leqslant 16$) associated with the second order magnetic transition at the Curie temperature and the first order martensitic transition were studied using magnetization measurements. The refrigeration capacity and magnetic entropy change were found to depend on the In concentration and reach a maximum value of refrigeration capacity of 280 J/kg with a magnetic entropy change of −6.8 J/kg K at 318 K for a magnetic field change of 5 T. These values of the magnetocaloric parameters are comparable to that of the largest values reported near the second order transition of metallic magnets near room temperature. © *2007 American Institute of Physics.* [DOI: 10.1063/1.2752720]

One of the topics of strong interest in recently discovered Ni$_{50}$Mn$_{50-x}$In$_x$ ferromagnetic Heusler alloys is the large value of the magnetocaloric effect (MCE) in the vicinity of the first order phase transition (FOPT), revealing their possible application as a working material in magnetic refrigerators.[1,2] These Heusler alloys possess at least two temperature induced phase transitions: the first order martensitic structural transition (T_M), accompanied by the change in magnetic state of the compound, and the ferromagnetic-paramagnetic transition at the Curie temperature (T_C) of the austenitic phase. The transition temperatures T_M and T_C are strongly dependent on the In concentration.[3] To date, most MCE studies of Ni$_{50}$Mn$_{50-x}$In$_x$ Heusler alloys have focused on ΔS_M and refrigeration capacity (RC) at the first order martensitic transition.[1,2,4,5] However, the metamagnetic character of magnetization at such transitions can result in large hysteresis losses and correspondingly small RC values. In contrast, the second order phase transition (SOPT) is characterized by a relatively small variation of the entropy but a large value of RC and low hysteresis losses.

In this letter, we report the MCE properties associated with both the second and the first order transitions in Ni$_{50}$Mn$_{50-x}$In$_x$ ($x = 15, 15.05, 15.2, 16$). The concentration of In was chosen for the possible existence of a coupled magnetostructural transition ($T_M = T_C$).[3] The ΔS_M and RC were found to vary with changing In concentration, and reaches a peak value of ≈ -7 J/kg K and 280 J/kg, respectively, at the second order transitions. These values are comparable to those found in the Gd based systems.[6,7]

Approximately 5 g polycrystalline Ni$_{50}$Mn$_{50-x}$In$_x$ ingots were prepared by conventional arc melting in a high purity argon atmosphere using $4N$ purity Ni, Mn, and In. The samples were annealed at 850 °C for 24 h under vacuum and slowly cooled down to room temperature. The phase purity and crystal structures were determined by powder x-ray diffraction using Cu $K\alpha$ radiation. Thermal expansion measurements were carried out using a capacitance dilatometer.[8] The magnetic properties were measured at temperatures ranging from 5 to 400 K, and at magnetic fields of up to 5 T, using a superconducting quantum interference device magnetometer (Quantum Design, Inc). The $\Delta S_M(T,H)$ was calculated from

isothermal magnetization curves using the Maxwell relation [Eq. (1)]. RC has been calculated by integrating the $\Delta S_M(T,H)$ curves over the full width at half maximum using relation (2).[9]

$$\Delta S_M(T,H) = \int_0^H \left(\frac{\partial M}{\partial T} \right)_H dH, \tag{1}$$

$$\mathrm{RC} = \int_{T_1}^{T_2} \Delta S_M dT. \tag{2}$$

The crystal structure of the Ni$_{50}$Mn$_{50-x}$In$_x$ compounds depends on x and changes from an austenitic cubic $Pm2m$ structure for $x = 16$ and 15.2 to a martensitic orthorhombic $Pmm2$ type structure for $x = 15$. For the sample with $x = 15.05$, the structure is of mixed phases (see Fig. 1). The crystal type and lattice constant with different In concentrations are presented in Table I. As expected, an increase in In concentration increases the cell volume of the austenitic phase.

All compounds undergo a martensitic transformation to the ferromagnetic austenitic phase at T_M (see Fig. 2), accompanied by jumplike variation in cell volume (see inset of Fig.
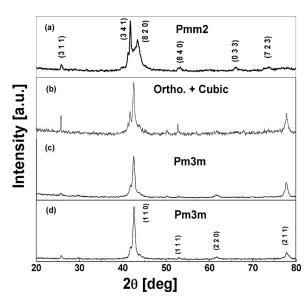

FIG. 1. Room temperature XRD patterns of Ni$_{50}$Mn$_{35-x}$In$_{50-x}$: (a) $x = 15$, (b) $x = 15.05$, (c) $x = 15.2$, and (d) $x = 16$.

a)Author to whom correspondence should be addressed; electronic mail: pathak@siu.edu

TABLE I. Crystallographic parameters, transition temperatures, and magnetocaloric parameters for $Ni_{50}Mn_{50-x}In_x$ in the vicinity of the second order and the first order transition at magnetic field change of 5 T.

x	Crystal type	Lattice parameter (Å)			T_C (K)	T_M (K)	ΔS_M at T_C (J/kg K)	RC at T_C (J/kg)	ΔS_M at T_M (J/kg K)	RC at T_M (J/kg)	Net RC at T_M (J/kg)
		a	b	c							
15	Pmm2	18.068	10.713	4.615	316	311	−5.7	123	35.8	167	57
15.05	Ortho+ cubic	3.000	3.000	3.000	328	282	−6.6	240	23	260	165
15.2	Pm3m	3.003	3.003	3.003	328	212	−7	224	13	236	196
16	Pm3m	3.006	3.006	3.006	325	143	−6.8	280	5.3	50	47.7

2). As the temperature increases further, the samples undergo a transition to the paramagnetic state at T_C. An increase in the In concentration results in a decrease in T_M, while T_C of the austenitic phase remains relatively constant (see Fig. 2 and Table I). This behavior agrees in general with previously reported data.[3,10]

Typical $M(H)$ curves for the $Ni_{50}Mn_{50-x}In_x$ system in the vicinity of T_C and T_M are shown for $x=15.05$ in Fig. 3. The transition at T_C is accompanied by a smooth transformation of $M(H)$ from the ferromagnetic to the paramagnetic shape, while jumplike changes in $M(H)$ with large hysteresis were observed for the transition at T_M.

The magnetic entropy changes (ΔS_M) calculated from the isothermal magnetization curves using Eq. (1) are shown in Fig. 4. Although this equation is meant for the second order magnetic transition, most often it has been employed to calculate ΔS_M in the vicinity of the first order phase transition which is justified in cases where problematic discontinuities are not present in the phase transition.[9] At the FOPT, the $Ni_{50}Mn_{50-x}In_x$ system exhibits positive ΔS_M with the peak ΔS_M value decreasing with increasing In concentration. The samples exhibit negative ΔS_M at the SOPT with little variation in the peak ΔS_M values with changing In concentration. At FOMT, the ΔS_M curve of the sample with $x=15.05$ shows extra peaks (large fluctuations) that are experimentally repeatable. As shown in Fig. 2, a large discontinuity (change) of magnetization occurs in a very narrow temperature range at the martensitic transition of the sample. Since the isothermal magnetization data were obtained in a 1 K temperature interval, the ΔS_M curve of the sample with

$x=15.05$ shows such fluctuations. These fluctuations disappear if a temperature interval of 3 K or more is used in obtaining the isothermal magnetization. Therefore, to avoid errors, the RC of the sample with $x=15.05$ was calculated from the ΔS_M curve obtained from isothermal magnetization curves obtained in 3 K interval (see the fitted curve of the sample with $x=15.05$ in Fig. 4). The ΔS_M and RC values for different In concentrations are presented in Table I. Magnetic hysteresis causes the thermal losses at the FOPT [see Fig. 3(b)]. This loss opposes the RC and is therefore an unwanted characteristic in a magnetocaloric system.[11] The estimated average loss, calculated from the hysteresis area of $M(H)$ for $x=15.05$ [see Fig. 3(b)], was found to be 95 J/kg. Therefore, the net RC calculated by subtracting average hysteresis loss from RC is found to be 165 J/kg for $x=15.05$. The net RC at T_M with different In concentrations are presented in Table I. The largest value of the net RC (280 J/kg) for the second order magnetic transition was found for $x=16$ at $T_C=325$ K, with $\Delta S_M \approx -6.8$ J/kg K at $\Delta H=5$ T. These values are comparable to those of rare earth based systems near room temperature.[6,7,12] Moreover, RC and ΔS_M associated with SOPT for $x=16$ are linearly dependent on magnetic field (see
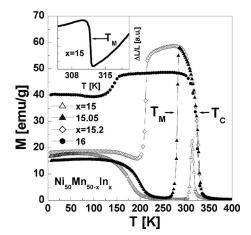

FIG. 2. Magnetization (M) vs temperature (T) at magnetic field (H) of 0.1 T for different In concentrations. (Inset) Thermal expansion of $Ni_{50}Mn_{35}In_{15}$ near the martensitic transition.
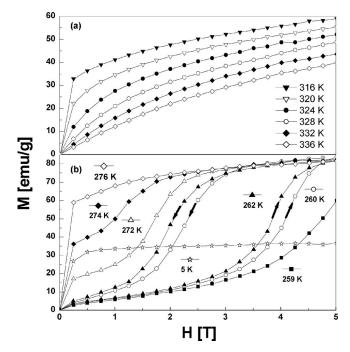

FIG. 3. Isothermal magnetization curves for $Ni_{50}Mn_{34.95}In_{15.05}$ in the vicinity of (a) the second order transition and (b) the first order martensitic transition.
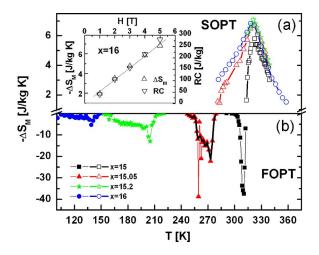
FIG. 4. (Color online) Magnetic entropy changes (ΔS_M) of $Ni_{50}Mn_{50-x}In_x$ at magnetic field (H) of 5 T in the vicinity of (a) the second order transition (open symbols) and (b) the first order martensitic transition (closed symbols).

inset of Fig. 4). Our other samples also show high values of RC near room temperature.

In conclusion, we have observed large values of ΔS_M accompanied with large hysteresis losses at the FOPT in $Ni_{50}Mn_{50-x}In_x$. The value of ΔS_M decreases in the SOPT; however, the $\Delta S_M(T)$ curves became broader and the largest value of the net RC was 280 J/kg for sample $x=16$ around room temperature for a magnetic field change of $0-5$ T. The observed RC and ΔS_M near T_C, and easily tunable transition temperature by the variation of In concentration, make $Ni_{50}Mn_{50-x}In_x$ system an attractive potential magnetic refrigerant material when compared to expensive rare earth based materials, as well as to potentially toxic alloys containing As, P, and Sb.

[1]Thorsten Krenke, Eyüp Duman, Mehmet Acet, Eberhard F. Wassermann, Xavier Moya, Lluís Mañosa, Antoni Planes, Emmanuelle Suard, and Bachir Ouladdiaf, Phys. Rev. B **75**, 104414 (2007).
[2]Z. D. Han, D. H. Wang, C. L. Zhang, S. L. Tang, B. X. Gu, and Y. W. Du, Appl. Phys. Lett. **89**, 182507 (2006).
[3]Y. Sutou, Y. Imano, N. Koeda, T. Omori, R. Kainuma, K. Ishida, and K. Oikawa, Appl. Phys. Lett. **85**, 4358 (2004).
[4]K. Oikawa, W. Ito, Y. Imano, Y. Sutou, R. Kainuma, K. Ishida, S. Okamoto, O. Kitakami, and T. Kanomata, Appl. Phys. Lett. **88**, 122507 (2006).
[5]V. K. Sharma, M. K. Chattopadhyay, and S. B. Roy, J. Phys. D **40**, 1869 (2007).
[6]A. Yucel, Y. Elerman, and S. Aksoy, Jr., J. Alloys Compd. **420**, 182 (2006).
[7]R. D. Shull, V. Provenzano, A. J. Shapiro, A. Fu, M. W. Lufaso, J. Karapetrova, G. Kletetschka, and V. Mikula, Jr., J. Appl. Phys. **99**, 08K908 (2006).
[8]M. O. Steinitz, J. Genossar, W. Schnepf, and D. A. Tindall, Rev. Sci. Instrum. **57**, 297 (1986).
[9]K. A. Gschneidner, Jr., V. K. Pecharsky, and A. O. Tsokol, Rep. Prog. Phys. **68**, 1479 (2005).
[10]Thorsten Krenke, Mehmet Acet, Eberhard F. Wassermann, Xavier Moya, Lluís Mañosa, and Antoni Planes, Phys. Rev. B **73**, 174413 (2006).
[11]Shane Stadler, Mahumd Khan, Joseph Mitchell, Naushad Ali, Angelo M. Gomes, Igor Dubenko, Armando Y. Takeuchi, and Alberto P. Guimarães, Appl. Phys. Lett. **88**, 192511 (2006).
[12]Manh-Huong Phan and Seong-Cho Yu, J. Magn. Magn. Mater. **308**, 325 (2007).